The Deacon Cell and the Other Meridional Cells of the Southern Ocean

KRISTOFER DÖÖS AND DAVID J. WEBB

Institute of Oceanographic Sciences, Wormley, Godalming, Surrey, United Kingdom

(Manuscript received 26 January 1993, in final form 18 June 1993)

ABSTRACT

The meridional circulation cells of the Southern Ocean are investigated using the results from a fine-resolution primitive equation model. Zonal integration along depth levels shows the classical series of meridional cells but integration along density layers shows a number of differences, including the virtual disappearance of the Deacon cell.

To investigate the differences, the meridional transport is calculated as a function of both density and depth. The results show that the Deacon cell is associated with systematic changes in the depth of density surfaces between the western boundary current region off South America and the return flow in the interior of the ocean. Water flowing on each density surface produces a meridional cell with a vertical excursion of a few hundred meters. These cells combine, without water crossing density surfaces, to produce a single integrated Deacon cell extending from the surface to below 2000 m.

The results also show that, at each latitude, water on each of the density surfaces in the upper layers of the ocean systematically transfers angular momentum from the shallowest depths at which it is found to deeper depths. In this way the torque, due the wind acting on the surface of the ocean, is transferred downward, in a series of steps between water masses of increasing density, until it is finally lost as a pressure torque acting on the ocean bottom topography.

1. Introduction

Data simulated by ocean general circulation models has an advantage, compared with data from observations, in that it is almost continuous in time and space. Because of this, it is possible to analyze numerical model data in ways that can give fresh insights into the ocean circulation.

One of the new features that model data has highlighted is the series of cells that become apparent when the ocean velocity field is integrated zonally to give the meridional streamfunction. In primitive equation models of the ocean, such plots are often used to illustrate the thermohaline circulation of the ocean. Examples are Bryan and Cox (1968), Holland (1971), and Gill and Bryan (1971). The latter model, which was a simple representation of the Southern Ocean from the equator to 70°S, showed a single thermohaline cell with a sinking region near Antarctica and a broad upwelling region north of 50°S.

More recently Manabe et al. (1990) found that the Southern Ocean had a much more complex structure (see Fig. 1). A similar cell was observed by Semtner and Chervin (1992). Between 30°S and 65°S Manabe et al. show the main cell circulating in a direction opposite to that of Gill and Bryan (1971). At the surface there is a strong northward Ekman transport driven by the westerly winds. The winds in their coupled ocean–atmosphere were weaker than those observed, but they were sufficient to produce a maximum transport of 20 Sv (1 Sv $\equiv 10^6$ m^3 s^{-1}) at 45°S. Between 30° and 45°S the water in the Ekman layer appears to sink to depths between 1 and 3 km. It then appears to flow southwards at this depth and rise almost vertically, north of 65°S, to complete the circulation. The circulation has become known as the Deacon cell (Bryan 1991).

Manabe et al. (1990) show four other cells in the Southern Ocean. The first of these extends from the surface to the bottom of the ocean close to Antarctica and is presumably associated with the formation of Antarctic Bottom Water. The second starts at 60°S in the deep ocean and extends northward across the equator. It shows northward flow at depths below 3500 m, with a return southward flow at middepths. The third is a shallow surface cell extending from 30°S to the equator and associated with the poleward Ekman transport driven by the trade winds. Finally, there is a branch of a Northern Hemisphere cell that extends south to 30°S at depths near 1500 m.

The dynamics of these cells is not well understood. Two of them involve Ekman layers driven by the trade winds and westerlies and may represent the ocean's response to these winds. At first sight, two of the other cells appear to be associated with the movement of Antarctic Bottom Water and North Atlantic Deep

Corresponding author address: Dr. Kristofer Döös, Institute of Oceanographic Sciences, Deacon Laboratory, Brook Road, Wormley, Surrey, UK GU8 5UB.

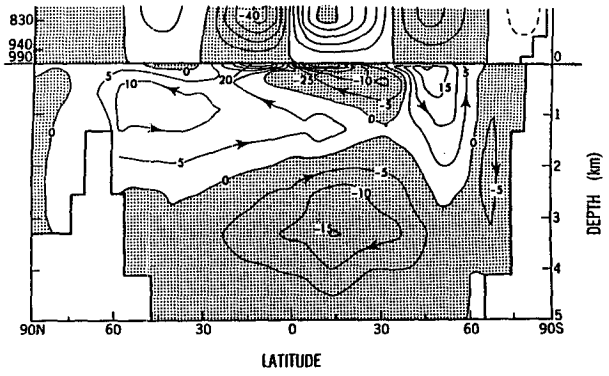

FIG. 1. Zonally integrated streamfunction from an equilibrium climate run of a coupled ocean–atmosphere model. [From Fig. 7 of Manabe et al. (1990), with permission.]

Water, but such inferences should be treated with care. As an example of how the meridional streamfunction can be misleading, in Fig. 1, the water flowing southward at a depth near 2500 m appears to sink near 40°S, whereas the North Atlantic Deep Water, with which the flow might be connected, does not do this.

The apparent vertical excursions of the water particles associated with these cells are large and also need to be explained. In the case of the Deacon cell near 30°S, surface water appears to be sinking to depths of 2 km or more in regions that are well stratified and in which, in field experiments, deep convection is not observed.

In this paper we investigate the meridional cells in more detail, making use of the results from FRAM (the U.K. Fine Resolution Antarctic Model), a high-resolution numerical model of the Southern Ocean (The FRAM Group 1991).

We find that because, at each level in the ocean, different water masses are often traveling in different directions, the flows illustrated by the meridional streamfunction are often poor approximations to the actual water particle movements in the model. However, we also find that the meridional streamfunction contains useful information on the transport of angular momentum by the ocean.

The results support Munk and Palmén's (1951) proposal that the Southern Ocean exports angular momentum to lower latitudes in the surface Ekman layer and imports it deeper in the water column. The results also show how the angular momentum may be advected vertically. The results do not support Johnson and Bryden's (1989) proposal that the surface Ekman layer is absent in the Southern Ocean and that an eddy form drag, resulting from a poleward transport of heat by eddies generated by baroclinic instability, produces the downward transfer of momentum.

2. The fine-resolution Antarctic model

FRAM was based on the Bryan–Cox–Semtner ocean model (Bryan 1969; Semtner 1974; Cox 1984) and covered the Southern Ocean from 24°S to Antarctica at a resolution of 0.25° in the north–south direction and 0.5° in the east–west direction. The model was initialized as a cold (−1.92°C), saline (36.6 psu), motionless fluid, and for the first 6 years of the model run, the temperature and salinity fields were dynamically relaxed to the annual mean Levitus (1982) data. For the first 2 years 160 days, the relaxation time was 180 days, in the top 140 m, and 540 days in the deeper levels. From then to 6 years, the relaxation time was 360 days throughout the model ocean. After 6 years relaxation was retained in the surface layer, to reflect the exchange of heat and fresh water with the atmosphere.

During the first 2 years, the model was run without any surface wind stress forcing. During the next six months, the wind stress field was increased linearly to the Hellerman and Rosenstein (1983) annual mean wind stress field. This was then used until the end of the 6-year spinup period. For the rest of the run, the Hellerman and Rosenstein (1983) monthly wind stress field was used.

FRAM ran for a total period of 16 model years, of which the last six have be chosen for detailed analysis. Although the potential energy of the model dropped slightly during the analysis period, it otherwise appears to be in a statistically steady state, with a well-developed eddy field and regular seasonal variations. During the analysis period, data from the model was archived at monthly intervals. The results presented in the paper are calculated by making time and space averages over the whole of this archived data.

3. The meridional circulation as a function of latitude and depth

The meridional circulation is traditionally represented as a function of latitude and depth. This has the advantage of producing a coherent picture of the circulation out of the confused jumble of flows and counterflows at different longitudes. However, because the detailed relationships between the velocity, density, temperature, and salinity fields are lost, the interpretation of the resulting meridional circulation field must be treated with care and not taken to be typical of the flows found near any particular longitude. Near 30°S, for example, where three ocean basins are found, the meridional circulation of the Indian Ocean is broadly speaking opposite to that of the Atlantic and Pacific oceans at all depths (Saunders and Thompson 1992).

Let $\psi(\theta, z)$ be the meridional streamfunction defined as a function of latitude θ, and depth z. If v is the meridional velocity, ϕ the longitude, and R the earth's radius, then

$$\psi(\theta, z) = \int_z^0 \int_0^{2\pi} v(\phi, \theta, z') R \cos\theta d\phi dz'. \quad (3.1)$$

The time-averaged streamfunction, obtained by integrating (3.1) over the six-year FRAM analysis period is shown in Fig. 2. The model shows four of the five cells illustrated by Manabe et al. (1990). The one that is missing is the deep convective cell near Antarctica. This probably occurs because the FRAM model did not form Antarctic Bottom Water.[1] The FRAM results also differ from those of Manabe et al. (1990) in that part of the circulation associated with the subpolar Ekman layer is also associated with the large Northern Hemisphere cell.

In FRAM, the northward flowing subpolar Ekman layer extends from Antarctica to 31°S, with a maximum transport of 31 Sv at 45°S. Of this, 16 Sv downwells between 45° and 36°S, flows south at depths of between 800 m and 2400 m and appears to upwell north of 57°S, the northern latitude of Drake Passage. This is the "Deacon cell" of Bryan (1991). The remaining 15 Sv sinks between 36° and 31°S. It flows out through the northern boundary of the model at depths between 200 m and 600 m and returns between 1600 m and 2400 m. It continues south under the Deacon cell and appears to upwell south of 57°S. We call this cell, associated with the thermohaline circulation, the "sub-polar cell."

The FRAM results show two other major cells. The first, a deep cell lying between 2400 m and the bottom, is similar in position and strength to that of Manabe et al. (1990). As with the other cells, this involves an apparent large vertical excursion of the water. The second, the sub-tropical cell, lies near the surface, near the northern boundary of the model. The cell is associated with the trade winds, which drive a southward flowing Ekman layer in the region. The water sinks before reaching 36° and returns northward in a shallow layer.

The meridional circulation and the conservation of angular momentum

Below the surface Ekman layer, the large-scale circulation is known to be approximately in geostrophic balance. Within the Ekman layer the vertical turbulent stress associated with the surface wind stress must also be included. Neglecting small terms, but including $\partial u/\partial t$, where u is the zonal velocity, the zonal momentum equation becomes

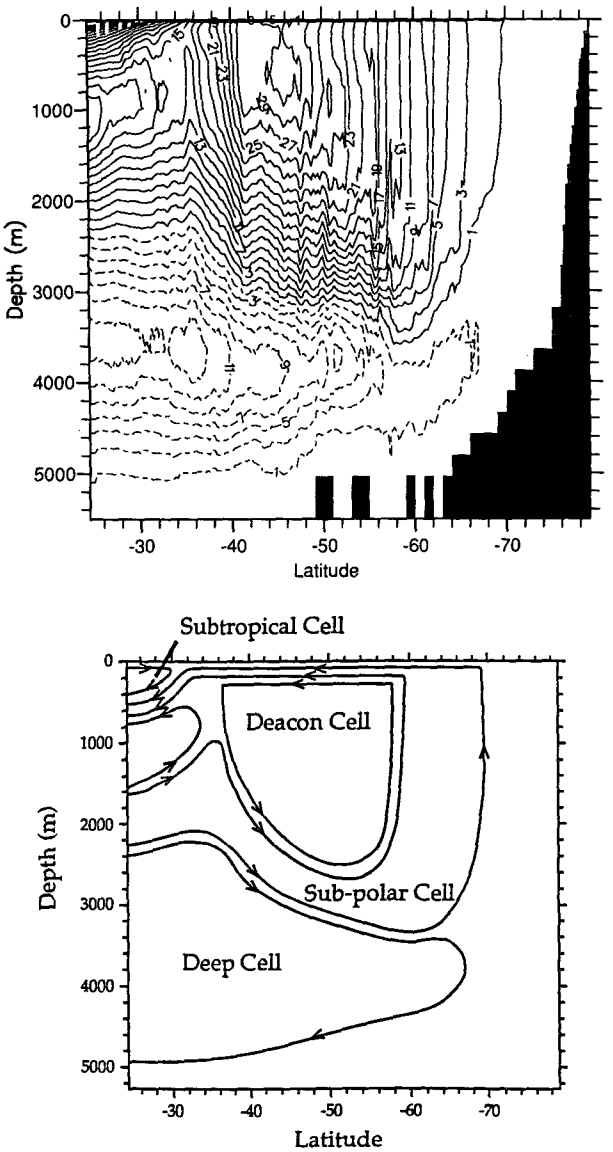

FIG. 2. (a) The meridional streamfunction from the FRAM model, where the zonal integration has been carried out at fixed depths. Units are in Sverdrups (1 Sv ≡ 10^6 m^3 s^{-1}). (b) Schematic showing the names and direction of flow of the different cells.

$$\rho \partial u/\partial t = \rho f v - \partial p/\partial x + \partial \tau^x/\partial z, \qquad (3.2)$$

where τ^x is the vertical turbulent stress. It equals the zonal wind stress at the surface of the ocean and decays rapidly to a "small" value at the bottom of the Ekman layer. Integrating the equation zonally and multiplying by $R\cos\theta$ gives the equation for conservation of angular momentum A_m:

$$\partial A_m/\partial t = R\cos\theta(\rho f V - (p_e - p_w) + \partial T^x/\partial z). \quad (3.3)$$

Averaged over a period of many inertial oscillations, both $\partial u/\partial t$ and $\partial A_m/\partial t$ in the above equations are small

[1] The lack of good observational data over the winter sea ice fields surrounding Antarctica makes it difficult to specify a good surface boundary condition for heat and fresh water. In the FRAM main run, a compromise boundary condition was used in which the temperature and salinity in the surface layer of the model was relaxed toward the mean annual Levitus dataset, using a one-year decay time. Because at high latitudes the Levitus data is biased toward summer conditions and because Antarctic Bottom Water needs winter conditions to form, Antarctic Bottom Water is not formed in the FRAM model.

compared with the other terms. Thus, from (3.3), for the time-averaged flow,

$$R\cos\theta(\rho f V - (p_e - p_w) + \partial T^x/\partial z) = 0. \quad (3.4)$$

Here T^x is the integrated stress term stemming from the zonal wind stress, and $(p_e - p_w)$ is the contribution due the solid earth applying pressure forces at the eastern and western boundaries of each ocean basin. The Coriolis term, $R\cos\theta f V$, where V is the zonally integrated meridional velocity, represents the torque arising from the change of potential angular momentum as water moves toward or away from the equator. Potential angular momentum is discussed further in the Appendix. Here V is also equal to the vertical derivative of the streamfunction [Eq. (3.1) and Fig. 2].

Interpreting Fig. 2 in terms of this equation, one sees that between Antarctica and 31°S, the torque due to the wind is transformed into potential angular momentum by the northward movement of the surface layer. Because of the way that potential angular momentum is a property of each water particle and depends only on its position, the meridional streamfunction contours can be considered as representing the mean paths by which potential angular momentum is conveyed around the ocean. As a result, the downwelling region of the cell is also the region where, on average, potential angular momentum is transferred downwards from the surface. Eventually it reaches levels where it can be lost to the solid Earth, via topographic pressure torques, in regions where the flow is southward.

An unexpected feature of the meridional circulation is that between 35° and 57°S, there is very little net meridional flow in the top 1000 m of the ocean, outside the Ekman layer. From (3.4), this implies that the mean zonal pressure gradient at these latitudes and depths is approximately zero despite the presence of continents, which could support a large pressure gradient. Farther south at the latitudes of Drake Passage (i.e., between 57° and 63°S) and between the surface and 1600-m depth, there is no effective zonal topographic barrier. In this region the mean zonal pressure gradient term must be zero and so, if (3.4) is still to hold, the meridional transport, outside the wind-effected surface layer, must be close to zero. This is confirmed by the model results. As shown in Fig. 2, upwelling occurs above 1600 m in this latitude band, but the meridional flow is negligible. Further confirmation comes from Stevens and Ivchenko (1993), who have carried out a detailed study of the balance of terms at the latitudes of Drake Passage. In the surface Ekman layer and at the level of topography, they find by integrating zonally that the primary balance is between the Coriolis term and either the wind stress or the bottom pressure torque. At intermediate depths they find a much smaller Coriolis term balanced by the small eddy transport terms, which were neglected in deriving (3.4).

These results from FRAM support Munk and Palmén's (1951) conjecture that the Southern Ocean exports angular momentum to lower latitudes near the surface and imports it deeper in the water column. Figure 2 indicates that the export of angular momentum at the surface is a result of the northward flow in the surface Ekman transport.

To confirm this, we can calculate the balance of forces integrated over the Ekman layer depth. This is given by

$$T_x = -\rho f V_e + \text{small terms}, \quad (3.5)$$

where V_e is the meridional velocity integrated zonally over the Ekman layer. Multiplying by $R\cos\theta$, gives the angular momentum form of the equation,

$$R\cos\theta T_x = -R\cos\theta\rho f V_e + \text{small terms}, \quad (3.6)$$

or (see Appendix),

$$R\cos\theta T_x = \rho \mathbf{V}_e \cdot \nabla((R\cos\theta)^2\Omega) + \text{small terms}. \quad (3.7)$$

The term on the left is the total torque due to the wind stress at each latitude, that on the right is the rate of change of potential angular momentum (both per unit distance in the meridional direction). The two sides of this equation are plotted in Fig. 3, with the Ekman transport taken to be the integrated velocity in the surface layer of the model relative to layer two. The good agreement between the two curves supports Munk and Palmén's conjecture because it shows that at each latitude in the FRAM model, the torque acting on the

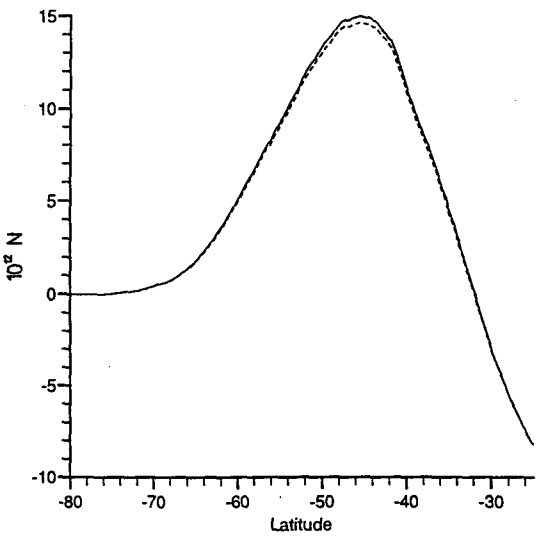

FIG. 3. The angular momentum torque, per unit distance in the meridional direction, due to the surface wind stress (solid line) compared to the torque associated with the northward transport in the surface Ekman layer (dashed line). The latter is obtained by integrating the northward velocity in the top model layer relative to the velocity in the next layer down.

ocean due to the wind is balanced almost entirely by the change in potential angular momentum of water in the surface layer.

At the latitudes of Drake Passage, a net zonal pressure gradient, and a geostrophically balanced meridional transport, can be supported at depths that intersect topography. This occurs at depths below 1600 m. Although there are gaps in the topographic barrier extending down to 3000 m, these can be spanned if there is an associated strong zonal current, the Antarctic Circumpolar Current (Webb 1993). Figure 2 shows that in the FRAM model, 14 Sv crosses all or part of Drake Passage in the band between 1600 m and 3000 m. In contrast, only 3 Sv of the subpolar cell water crosses the whole of Drake Passage below this band.

4. The meridional circulation as a function of latitude and density

The disadvantage of working with a meridional streamfunction defined as a function of latitude and depth, is that it is tempting to treat the horizontal and vertical flows that it illustrates as flows along and across density surfaces. For this reason, in this section, we introduce a second streamfunction defined as a function of latitude and potential density.[2] Let,

$$\psi(\theta, \rho) = \int_0^{2\pi} \int_{z(\phi,\theta,\rho)}^{0} v(\phi, \theta, z') R \cos\theta dz' d\phi, \quad (4.1)$$

where $z(\phi, \theta, \rho)$ is the depth of the isopycnal ρ.

The resulting streamfunction for the FRAM model is shown in Fig. 4. This was calculated, as indicated in (4.1), by first integrating the meridional velocities from the surface to the appropriate density surface and then integrating zonally. As a result the north–south transport between two density surfaces at a given latitude is given correctly by the difference in the streamfunction. However, the corresponding difference in the streamfunction at different latitudes but on the same density layer only represents a mean flux of water across the layer for an ocean in thermodynamic steady state. If the system is not in a steady state, then a nonzero value may represent the situation where, at intermediate latitudes, water of lower density is replacing or being replaced by water of greater density.

The results obtained by plotting the streamfunction relative to density surfaces give a very different view of the circulation. The Deacon cell is virtually missing and the main features involve flows in and out of the northern boundary. Net inflows occur at densities less than 25.1 kg m^{-3} and between 27.2 and 27.85 kg m^{-3}. Net outflows occur at densities between 25.1 and 27.2 kg m^{-3} and below 27.85 kg m^{-3}.

[2] Except where stated, the density used is ρ_0, the potential density relative to surface pressure. Following standard practice the values quoted and plotted are the full density minus 1000 kg m^{-3}.

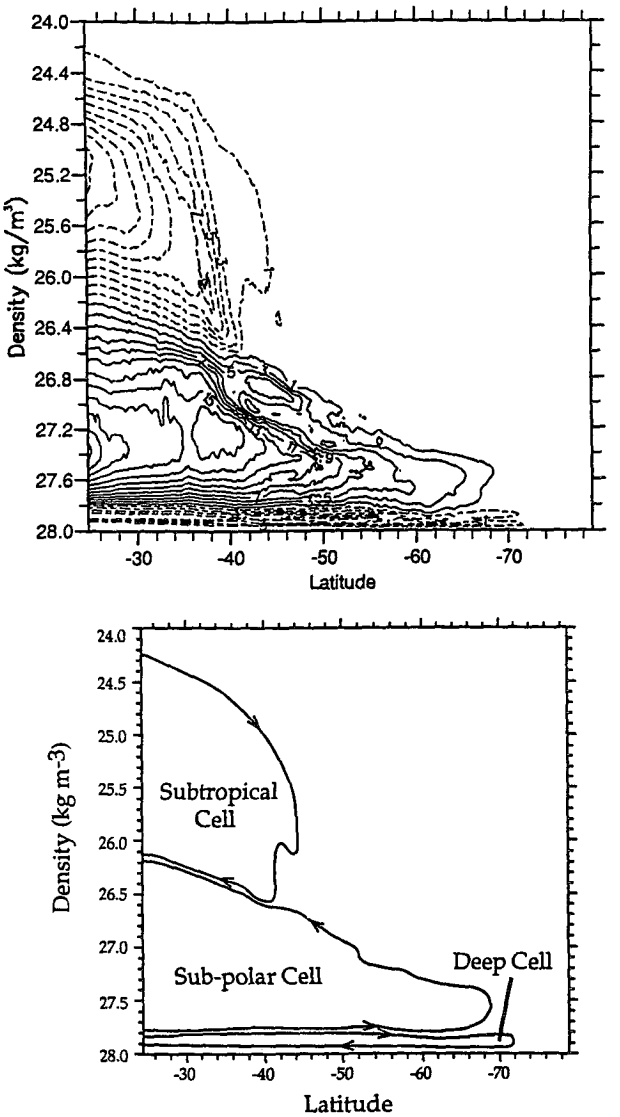

FIG. 4. (a) The meridional streamfunction from the FRAM model, where the zonal integration has been carried out on layers of constant potential density ρ_0 (units: Sv). (b) Schematic showing the names and direction of flow of the different cells.

To help in the interpretation of Figs. 2 and 4, the mean position of the density surfaces in the FRAM model are plotted in Fig. 5a and the streamfunction obtained by transforming the density coordinate of Fig. 4 to the corresponding depth of Fig. 5a, is plotted in Fig. 5b. As before, the figures should be treated with care as, for a given longitude, the actual depth of a density surface may differ from the mean position by many hundreds of meters.

The inflow of water at densities less than 25.1 kg m^{-3} is readily identified as being the near-surface waters of the subtropical gyre. The total circulation of the cell is 19 Sv, the same transport as in the subtropical cell of Fig. 2. In this case the new meridional stream function

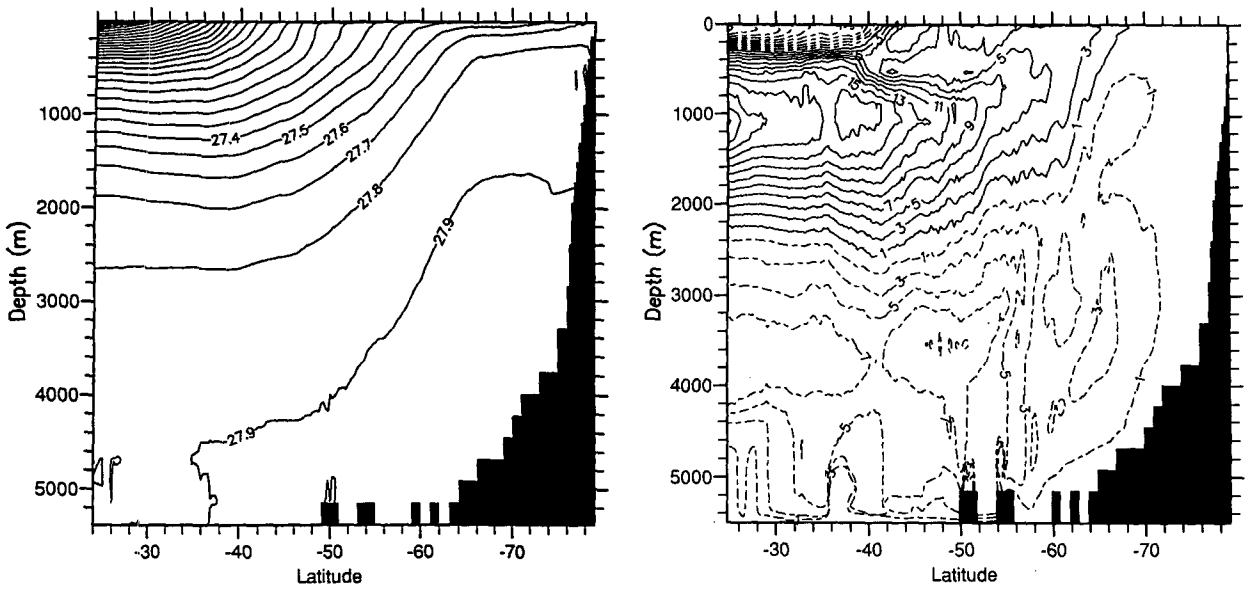

FIG. 5. (a) The zonal-averaged potential density ρ_0, in the FRAM model.
(b) The meridional streamfunction $\psi(\theta, \rho)$ transformed onto the mean density surfaces.

gives little new information. However within this cell, as in some of the others, the details of the flow are quite complex and differ between the different basins. [The three-dimensional structures are described in more detail in Döös (1993).]

Below the subtropical cell, the second major cell has an inflow region with densities corresponding approximately to North Atlantic Deep Water and outflow corresponding to Antarctic Intermediate Water. The transport through the northern boundary of this cell is 23 Sv. This flows southward, with little change in density, until upwelling brings it to the surface. There, changes in density can readily occur due to the exchange of heat and fresh water with the atmosphere. In Fig. 4 the surface is not represented as one specific isopycnal but as a range of values covering all the surface densities found at a particular latitude.

The water mass properties of the cell are similar to those expected of the subpolar cell of Fig. 2. The latitudinal extents are also similar and at 34°S, just north of the downwelling region of Fig. 2, so are the transports, 15 Sv in Fig. 2 and 17 Sv in Fig. 4. However, there are important differences. The downwelling branch of the Deacon cell is not found in the streamfunction defined on density surfaces (Fig. 4), and the transport in the cell drops off rapidly from a value of 17 Sv at 40°S, to only 5 Sv at 57°S, the northern latitude of Drake Passage. In contrast, the streamfunction on depth surfaces (Fig. 2), shows a transport of 31 Sv at 44°S, with 14 Sv upwelling north of 57°S and 17 Sv at the latitudes of Drake Passage and to the south.

Once at the surface the water is carried northward by the Ekman transport and slowly decreases in density due to buoyancy input from the atmosphere. This gives a cross-isopycnal flow illustrated by the increasing thickness of the cell toward the north. Thus, the 1 Sv contour corresponds to a density of 27.5 at 68°S, but this has reduced to 26.7 at 40°S. An analysis of the buoyancy inputs in the surface layer of the model has shown that the change in buoyancy is due to a freshwater input of 0.4 Sv. In practice this will involve both precipitation and melting sea ice. As the water in the cell flows north of 38°S, the picture is complicated by interference with the subtropical cell. The water masses in both cells show a decrease in density as they flow north. As mixing would tend on average to increase the density, the decrease is most likely to be a result of continued buoyancy input at the surface.

Below these two cells is a deep cell with a flux of 9 Sv at the northern boundary. The potential density ρ_0 of the inflowing and outflowing water masses is approximately 27.8 and 27.9 kg m^{-3}. A feature of this cell is the very small change in the density over large ranges of latitude. To confirm the flows in this cell, in Fig. 6 the streamfunction relative to density surfaces has been replotted using potential densities relative to 3000 m. In this more accurate calculation the transport in the cell is found to be 16 Sv at the northern boundary and to decrease to 10 Sv at 50°S. The more accurate calculation also shows a larger change in density between the inflow and outflow regions.

The deep cell is tentatively identified with the deep circulation field of Fig. 2 and with inflow of North Atlantic Deep Water and outflow of Antarctic Bottom Water. However, as has been discussed previously, such an identification should be treated with care.

There are some other noticable differences in the flow patterns shown by Figs. 4a and 6, especially near

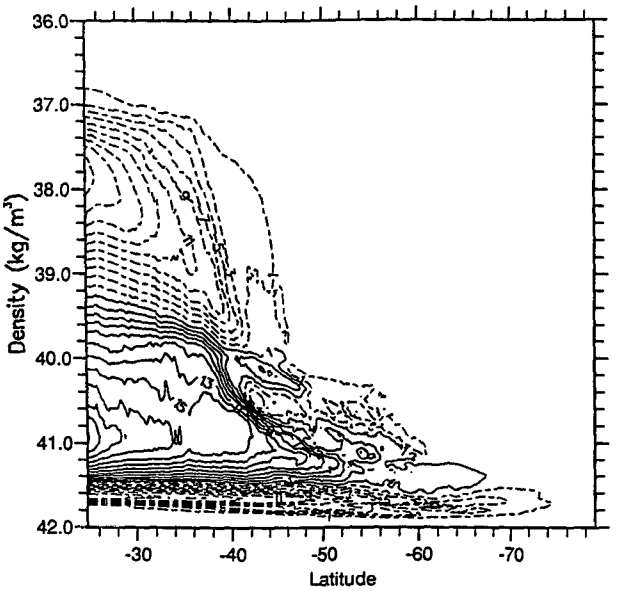

FIG. 6. The meridional streamfunction (in Sv) from the FRAM model, where the zonal integration has been carried out on layers of constant potential density ρ_{3000} (relative to the pressure at 3000 m).

the southern end of the range occupied by each density surface. Reference to Fig. 5a shows that these are mainly associated with flows occurring near the surface of the ocean for which Fig. 4a gives the most accurate picture.

A number of the small-scale circulation features warrant further study in the future. These include the recirculation region centered at density 26.9 kg m^{-3} and latitude 44°S, and the adjacent region of steeply sloping stream lines at 26.9 kg m^{-3} and latitude 39°S. These features, which both lie in the subpolar cell, may be related to features in the subpolar cell at the same latitudes, namely, the meander in the −1 Sv contour at density 26.0, latitude 44°S and the steeply sloping stream lines at 26.0 kg m^{-3}, latitude 39°S.

The missing Deacon cell

The most important difference between the two meridional streamfunction representations is that, when the flow is referred to density surfaces, the Deacon cell virtually disappears. There is a small downwelling branch at 36°S, following the 17 Sv contour of Fig. 4a, with a maximum transport of 2 Sv that could be identified as part of a Deacon cell. However, it is weak and may be part of the background noise. If it is a real feature, it is balanced by the adjacent upwelling branch at 36°S. The implications of this are important. First, although both Figs. 1 and 2 show that there is a total flux of 16 Sv downwelling near 40°S to depths near 2000 m, little of this flow can be crossing density surfaces or it would show up in Fig. 4. Instead, the bulk of the Deacon cell must be produced by a circulation in which the water particles involved do not change their density. For this reason it is sensible to be more specific in the definitions of the subpolar and Deacon cells. We therefore define the "Deacon cell" to represent that part of the meridional gyre associated with the Southern Hemisphere westerlies, in which the water particles undergo no changes in density and define the "subpolar cell" to correspond to that part involved in the thermohaline circulation, in which density changes do occur.

With these revised definitions, the flow in the subpolar cell is exactly that given by the streamfunction defined relative to density surfaces. Figure 4 shows that the total transport in the cell at 40°S is 17 Sv, of which 12 Sv upwells north of 57°S, the northern latitude of Drake Passage, and 5 Sv upwells farther south. The Deacon cell transport has to be estimated from the differences between Fig. 2 and Fig. 4. The comparison indicates that within the Deacon cell 16 Sv downwells near 38°S, 6 Sv upwells between there and 57°S, and the remaining 10 Sv upwells farther south.

Given these results, the most promising explanation for the existence of the Deacon cell is a geometrical one. Suppose the northward and southward transports on each density level are equal, but, because the density levels slope from east to west, these occur on average at different depths. A zonal integration along density levels will then give no net flow, but an integration at constant depth will give a Deacon cell–type circulation.

To investigate whether this is true for the Southern Ocean we need to investigate both the depth and density at which the meridional flows are occurring. This is done in the next section.

5. The meridional circulation as a function of both depth and density

To investigate the link between the two representations, we defined a meridional transport as a function of both depth and density. Let

$$V(\theta, z, \rho) = \int_0^{2\pi} v(\phi, \theta, z) \times \delta(\rho_0(\phi, \theta, z) - \rho) R \cos\theta d\phi, \quad (5.1)$$

ρ_0 is the potential density relative to the surface pressure and δ is the Dirac delta function defined so that,

$$\int \delta(x) f(x) dx = f(0).$$

Here $V(\theta, z, \rho)$ is related to the two meridional streamfunction representations by

$$\psi(\theta, z) = \int_z^0 \int_0^\infty V(\theta, z', \rho) d\rho dz' \quad (5.2)$$

$$\psi(\theta, \rho) = \int_0^\rho \int_{-H}^0 V(\theta, z, \rho') dz d\rho', \quad (5.3)$$

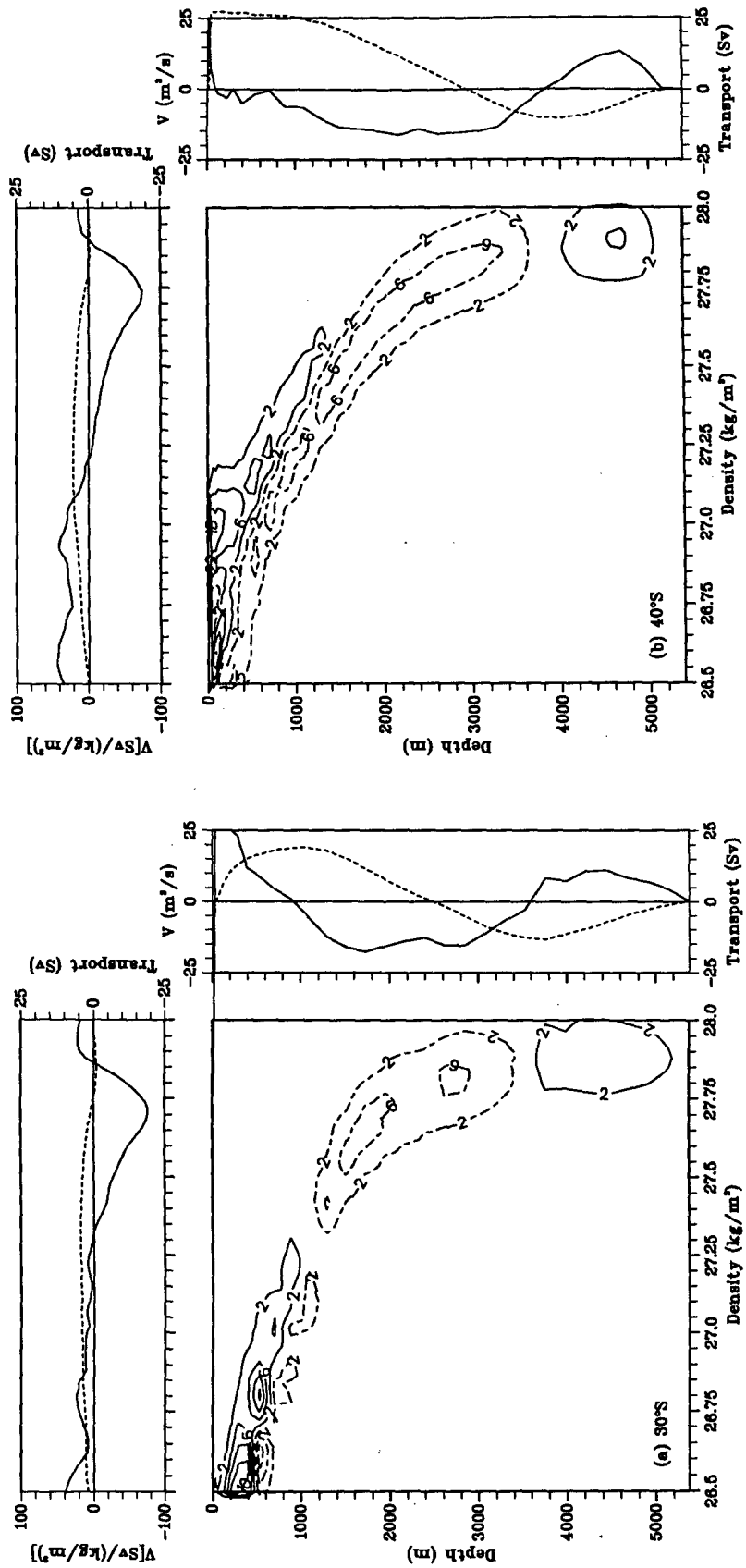

FIG. 7. The zonally integrated meridional velocity as a function of both depth and density, $(V(\theta, z, \rho)$ [see Eq. (5.1)], at (a) 30°S, (b) 40°S, (c) 50°S, and (d) 60°S. Solid lines correspond to positive transports, dotted lines to negative transports. Units are in 10^4 m^5 kg^{-1} s^{-1} (equal to 0.01 Sv per meter depth and per unit density). In the small figure to the right of each main figure, the solid line is the transport per unit meter depth obtained by integrating $V(\theta, z, \rho)$ with respect to ρ. In the small figure above each main figure, the solid line

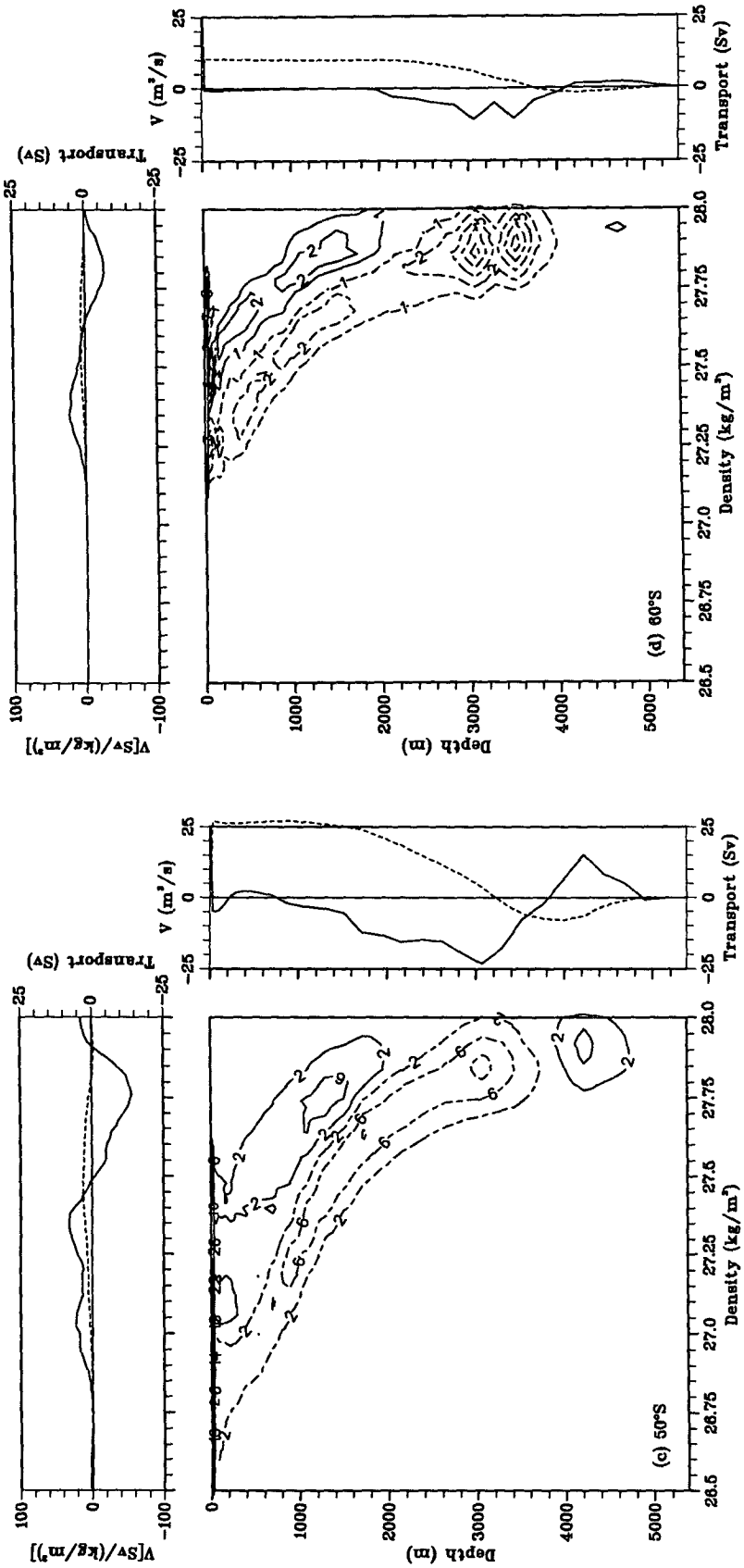

FIG. 7. (*Continued*) is the transport per unit density obtained by integrating $V(\theta, z, \rho)$ with respect to z. In both these figures the dotted lines give the integrated transports (in Sv). They correspond to sections through Figs. 2a and 4a, respectively.

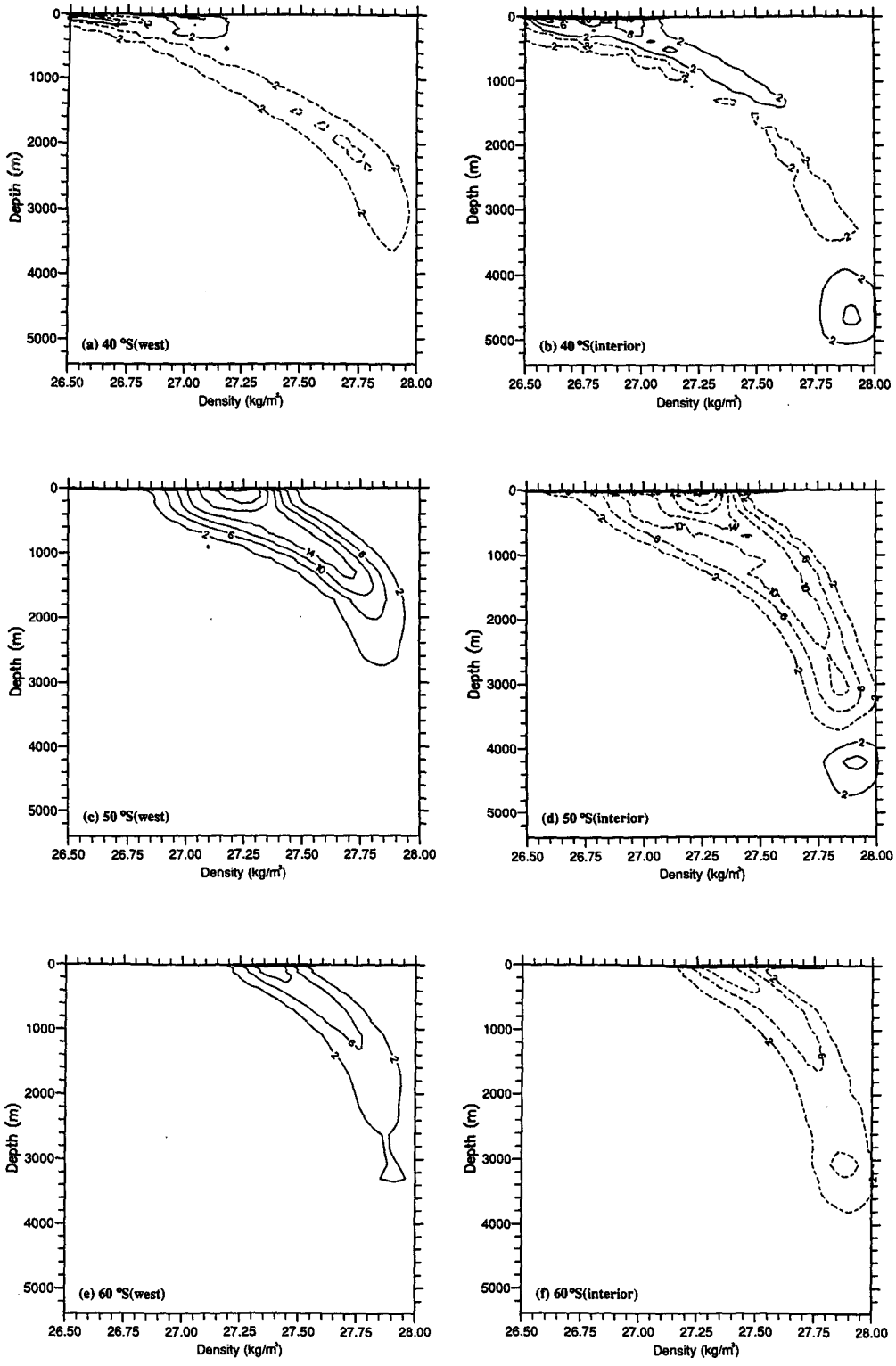
Depth (m)
Density (kg/m³)
(a) 40 °S(west)
(b) 40 °S(interior)
(c) 50 °S(west)
(d) 50 °S(interior)
(e) 60 °S(west)
(f) 60 °S(interior)

where H is the depth of the ocean.

The transports $V(\theta, z, \rho)$ at the latitudes 30°S, 40°S, 50°S, and 60°S are shown in Fig. 7. Also shown are the integrated transports and streamfunctions plotted as a function of both depth and density. The two streamfunctions are equivalent to sections taken from Figs. 2a and 4a. The results show that at 40°S, 50°S, and 60°S there is a clear double structure in the flow field, with bands of northward and southward flowing water at the same density extending from near the surface to below 2000 m. At a given depth, the northward flowing water is more dense than that flowing south. At a given density, the northward flowing water is at a shallower depth than that flowing south.

Above 2000 m, the double banded structure means that within each depth or density band the northward and southward transports tend to cancel out. This is most noticeable at 60°S, where between the Ekman layer and 2000 m, the net flow at each depth is almost zero. In the deep water, the main feature is a southward flow of water with densities centered on 27.8 kg m^{-3} at depths near 3000 m and a return flow of water with densities centered on 27.9 kg m^{-3} at depths near 4500 m.

a. *The angular momentum staircase and the Deacon cell*

At 60°S (Fig. 7d), there is a net northwards transport in the surface layers. The streamfunction on density surfaces shows that this is concentrated in water masses with densities near 27.3 kg m^{-3}. Some of the 27.3 kg m^{-3} water is lost to the north, but the rest returns south at a depth of 500 m. The total transport at 500 m is zero, so the potential angular momentum released by the southward flowing water must be absorbed by an equal amount of water moving north. Figure 7d shows that this northward moving water has densities near 27.6 kg m^{-3}. The 27.6 kg m^{-3} water returns south at 1500 m, again releasing its potential angular momentum. This is absorbed by northward flowing water with a density of 27.85 kg m^{-3}, which itself finally returns at depths near 3000 m, a depth at which there is no compensating flow. The potential angular momentum it releases must therefore be converted into a pressure torque acting on the topography.

The double-banded structure in Fig. 7d can be thought of as representing a staircase that transfers potential angular momentum from the surface Ekman layer to the level of the bottom topography. Potential angular momentum is carried from one level to the next by water sinking to the north of the section. As the water returns south its potential angular momentum is released, via the Coriolis term, and transferred to denser water via the horizontal pressure gradient (Appendix). This in turn carries the potential angular momentum to even deeper levels.[3]

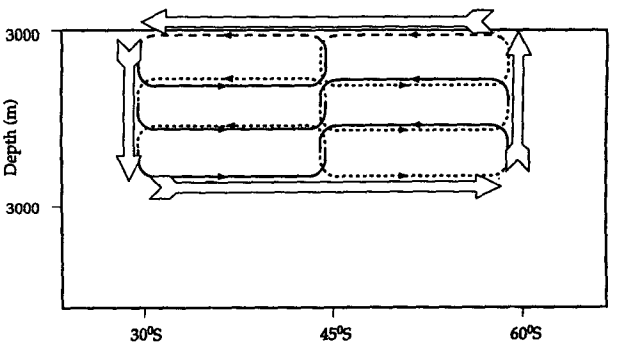

FIG. 9. A schematic view of the Deacon cell. The cells represent the circulation on isopycnals in the subtropical gyres to the north, and in the Antarctic Circumpolar Current to the south. The solid lines represent flows in the western boundary current region off South America, dashed lines represent flows in the rest of the ocean, and long dashes flows in the surface Ekman layer. The large arrows represent the Deacon cell, which results from integrating the flows zonally on depth levels.

At 60°S part of the Ekman flow, with densities near 27.3 kg m^{-3}, is lost to the north and is not involved in the staircase process. It eventually returns near 3000 m but with a density that has been increased to 27.8 kg m^{-3}. This flow also results in a transfer of angular momentum from the surface to the topography but it occurs as part of the thermohaline circulation.

At 50°S and 40°S similar double-banded structures are found, so at these latitudes angular momentum is also transferred downward by the staircase process. At these latitudes there is also a small net southward flow between the surface and 2000 m but this is generally smaller than the flows involved in the staircase process. At 30°S, there is still a remnant of the double band structure above 1000 m but at greater depths it has disappeared.

These results indicate that the staircase mechanism is involved in the vertical transfer of angular momentum over a large area of the Southern Ocean. The main area in which potential angular momentum is advected downward is between 36° and 41°S, in the region of

[3] An analytical model of this occurring in a double gyre ocean has been developed by Döös (1994).

FIG. 8. As in Fig. 6 but with a zonal integration split up in to two regions, one South American western boundary region (70°W to 50°W) and one interior region (50°W to 70°W). (a) 40°S (west), (b) 40°S (interior), (c) 50°S (west), (d) 50°S (interior), (e) 60°S (west), (f) 60°S (interior).

the downwelling branch of the Deacon cell (Fig. 2). Water on each density surface advects potential angular momentum downward only a few hundred meters, but the combined effect takes it from the surface to depths below 2000 m.

b. *The longitudinal distribution of the main flows*

To identify the longitudes at which the northward and southward flows occur, the calculation of $V(\theta, z, \rho)$ has been split into a western boundary contribution running from the South American coastline, near 70°W, to 50°W and an interior contribution covering the rest of the ocean. The resulting figures for the latitudes 40°S, 50°S, and 60°S are shown in Fig. 8. The sum of the western boundary and the interior contributions gives the same global result as shown in Fig. 7.

At 50°S in the western boundary region there are only northward flows. These must correspond to water carried by the Falkland Current. In the interior at the same latitude the net transport is southward except for a small region at the bottom of the ocean. This southward transport appears to be due to the Antarctic Circumpolar Current, which on average flows southward in this region. For water of a given density, the northward flow in the Falkland Current occurs at a shallower depth than the southward flow in the interior region. This results, in the global zonal integration (Fig. 7c) in the double-band structure.

Despite the lack of a meridional boundary at 60°S, the picture is qualitatively much the same as at 50°S. The transport is weaker here and the northward deep current in the interior has disappeared. Another feature is that the difference in the depths of the northward and southward flows is less at 60° than at 50°S. As a result when the two flows are added (Fig. 7d), the relative magnitude of the total is smaller.

At 40°S the positions of the northern and southern transports are reversed. The flow in the western boundary current is southward and corresponds to the direction of the Brazil Current (Fig. 8a). Above 1500 m, in the rest of the ocean (primarily of the interior part of the subtropical gyres), the net flow is northward (Fig. 8b). The results show that whereas the Deacon cell of Fig. 2 varies smoothly across the latitudes of the Brazil and Falkland Current confluence zone, the actual details of the mechanism involved change significantly.

In mathematical terms the horizontal transfer of angular momentum between water masses of different densities can be described as an eddy form drag. However, these are not the small-scale eddies of Johnson and Bryden (1989). They are not associated with baroclinic instability, the north–south flows do not transfer momentum in the vertical and they need not transfer heat meridionally. Instead the mathematical "eddy" term results from the large-scale circulation of the subtropical gyre and the large-scale meanders and changes in latitude of the path of the Antarctic Circumpolar Current.

Our final picture of the Deacon cell is shown schematically in Fig. 9. Two sets of cell are involved in transferring the torque applied to the ocean surface by the wind, downward to depths below 2000 m. One set of cells is associated with the Antarctic Circumpolar Current with, below the Ekman layer, the shallower northward flows occurring in the Falkland Current. The other set is associated with the subtropical gyres with the deeper southward flows occurring mainly in the Brazil Current region. It should be emphasised that Fig. 9 is a simplified schematic view and that many details have been left out. For example, as shown in Figs. 7b–d, at each latitude more than one density surface outcrops in the Ekman layer. However, the figure helps to illustrate that when the transports of all the cells are integrated on depth levels, instead of on density levels, they combine to produce a single large scale, smoothly varying, Deacon cell.

6. Conclusions

Using the results from a fine-resolution model of the Southern Ocean, we have shown that there are major differences in the meridional streamfunction depending on whether it is calculated by integrating along level surfaces or density surfaces. The most striking difference between the two representations is that the Deacon cell, found in the integration on depth levels, virtually disappears when integrating along the density surfaces. In particular, the Deacon cell downwelling that occurs near 40°S is not a cross-isopycnal flow.

The differences have been investigated and it has been found that in the region of the Deacon cell, a significant fraction of the angular momentum absorbed from the wind is transferred downward by a two-stage process that does not involve the thermohaline circulation. In the first stage, water particles that have absorbed potential angular momentum when moving northward sink to a lower level and return south without any change in density. In the second stage, the southward moving particles lose their potential angular momentum via the Coriolis term and transfer it to denser water traveling northward at the same depth via the horizontal pressure gradient. The two processes are then repeated.

Within the Deacon cell there are large northward and southward transports of water with different densities at the same level. However, these are almost equal in magnitude, so that when the meridional streamfunction is calculated relative to depth levels, the transport through the region appears small.

At the northern and southern limits of the Deacon cell, the water in each density layer moves vertically a few hundred meters. These small depth changes are correlated so that when transport calculations are made

relative to depth levels, the meridional streamfunction contours show changes in depth of 2000 m or more.

It has also been shown that in the northern part of the Deacon cell, the main flows involved are the Brazil Current in which the water flows south, at relatively deep levels, and the gyre recirculation region, in which the same density water flows north at a shallower depth. In the southern part of the Deacon Cell, the two main flows involved are the Falkland Current, in which the water flows north at a relatively shallow depth, and the remainder of the Antarctic Circumpolar Current, in which the same density water flows south at a greater depth.

Acknowledgments. We would like to acknowledge the helpful comments of members of the FRAM group, Dr. David Straub, and Dr. Peter Saunders on an earlier draft of this manuscript.

APPENDIX

Conservation of Angular Momentum and the Coriolis Term

In this study we make use of the fact that, in a rotating coordinate system, north–south flows in the ocean change the potential angular momentum of the water involved and that the torque required to produce these changes give rise to the Coriolis terms in the zonal momentum equation. Although these properties are straightforward to derive, this is not done in standard texts (but see Straub 1992). For clarity we do so here.

Consider a coordinate system rotating about the origin with angular velocity Ω. If an element of fluid at point $\mathbf{r}$ has velocity $\mathbf{v}$ (in the rotating system), the absolute angular momentum $\mathbf{L}$, per unit volume, is

$$L = \rho \mathbf{r} \times (\Omega \times \mathbf{r} + v). \tag{A.1}$$

If a force $\mathbf{F}$ is applied to the fluid element, then

$$d\mathbf{L}/dt = \mathbf{r} \times \mathbf{F}. \tag{A.2}$$

In a spherical coordinate system, like the earth's, if a water particle position is defined by its radial distance r, latitude θ and longitude ϕ, then its velocity vector $\mathbf{v}(u, v, w)$ is equal to $(r\cos\theta\partial\phi/\partial t, r\partial\theta/\partial t, \partial r/\partial t)$. For the component of $\mathbf{L}$ parallel to the axis of rotation,

$$L_z = \rho r \cos\theta u + \rho\Omega(r\cos\theta)^2, \tag{A.3}$$

and

$$dL_z/dt = r\cos\theta F_\phi, \tag{A.4}$$

where F_ϕ is the zonal component of $\mathbf{F}$.

In (A.3), the first term on the right is the angular momentum relative to the rotating frame of reference. The second is the correction required to give conservation of absolute angular momentum. To an observer in the rotating frame of reference, it depends only on the particle position and so behaves as "potential" angular momentum. Potential angular momentum is stored when applied torques cause the elements of fluid to move away from the axis of rotation and is released when the elements return crossing the same distance from the axis of rotation.

Because it is $(r\cos\theta)$ and not r that has to be the same, a torque which generates potential angular momentum at one level in the ocean can be balanced by a torque which absorbs the same potential angular momentum at a different depth but at the same distance from the earth's axis.

Discussions of the Coriolis terms in the equations of motion usually make the general statement that they are terms that arise in transforming from a nonrotating to rotating frame of reference. To illustrate that in the zonal momentum equation, the Coriolis term arises specifically from the changes in potential angular momentum, we derive the zonal momentum equation from (A.4).

Assuming that the density is constant, replacing the operator d/dt by $\partial/\partial t + (\mathbf{u}\cdot\nabla)$ and substituting for L_z from (A.3), the rate of change of total angular momentum is

$$\rho(\partial/\partial t(r\cos\theta u) + (\mathbf{u}\cdot\nabla)(r\cos\theta u) + (\mathbf{u}\cdot\nabla)[(r\cos\theta)^2\Omega)] = r\cos\theta\mathbf{F}_\phi. \tag{A.5}$$

Dividing by $(r\cos\theta)$ and expanding, gives the standard zonal momentum equation,

$$\rho\{\partial u/\partial t + (\mathbf{u}\cdot\nabla)u + [u/(r\cos\theta)](\mathbf{u}\cdot\nabla)(r\cos\theta) + 2\Omega(w\cos\theta - v\sin\theta)\} = \mathbf{F}_\phi. \tag{A.6}$$

The first three terms in this equation come from the relative angular momentum terms in (A.3) and (A.5). The first and second are the standard time derivative and advection terms. The third, often called the inertial term, arises from the curvature of the spherical coordinate system.

The two Coriolis terms in (A.6) come from the potential angular momentum components of (A.3) and (A.5). The first depends on the vertical velocity w, the second on the northward velocity v. The fact that the equation can be derived in this way means that, in the zonal direction, the Coriolis force is the direct result of the loss or gain of potential angular momentum.

The Bryan–Cox–Semtner ocean model, used in the present study, neglects the horizontal component of the Coriolis term. This is equivalent to defining the potential angular momentum as a function of latitude only. In such a model, water can sink vertically (instead of parallel to the earth's axis), without changing its potential angular momentum or experiencing a Coriolis force. Water that gains potential angular momentum by changing its latitude can lose it at a different depth by crossing back across the same latitude (instead of crossing the same distance from the earth's axis).

REFERENCES

Bryan, K., 1969: A numerical method for the study of the circulation of the World Ocean. *J. Comput. Phys.*, **4**, 347–376.

——, 1991: Ocean circulation models. *Strategies for Future Climate Research*, M. Latif, Ed., Max-Planck Institut für Meteorologie, 265–286.

——, and M. D. Cox, 1968: A nonlinear model of an ocean driven by wind and differential heating. Part 1: Description of the three-dimensional velocity and density fields. *J. Atmos. Sci.*, **25**, 945–967.

Cox, M. D., 1984: A primitive equation, 3-dimensional model of the ocean. GFDL Ocean Group Tech. Rep. No. 1, 143 pp.

Döös, K., 1993: The water mass exchange between the three oceans through the Southern Ocean simulated by FRAM. Unpublished manuscript.

——, 1994: Semi-analytical simulation of the meridional cells in the Southern Ocean. *J. Phys. Oceanogr.*, **24**, in press.

The FRAM Group [Webb, D. J., and others], 1991: An eddy-resolving model of the Southern Ocean. *Eos*, **72**(15), 169, 174–175.

Gill, A. E., and K. Bryan, 1971: Effects of geometry on the circulation of a three dimensional Southern Hemisphere ocean model. *Deep-Sea Res.*, **18**, 685–721.

Hellerman, S., and M. Rosenstein, 1983: Normal monthly wind stress over the world with error estimates. *J. Phys. Oceanogr.*, **13**, 1093–1104.

Holland, W. R., 1971: Oceanic tracer distributions. Part 1: A preliminary numerical experiment. *Tellus*, **23**, 371–392.

Johnson, G. C., and H. L. Bryden, 1989: On the size of the Antarctic Circumpolar Current. *Deep-Sea Res.*, **36**(1), 39–53.

Levitus, S., 1982: *Climatological Atlas of the World Ocean.* NOAA Prof. Paper No. 13, Geophysical Fluid Dynamics Laboratory, Princeton University, N.J., 173 pp.

Manabe, S., K. Bryan, and M. J. Spelman, 1990: Transient response of a global ocean–atmosphere model to a doubling of atmospheric carbon dioxide. *J. Phys. Oceanogr.*, **20**(6), 722–749.

Munk, W. H., and E. Palmén, 1951: Note on the dynamics of the Antarctic Circumpolar Current. *Tellus*, **3**, 53–55.

Saunders, P. M., and S. R. Thompson, 1992: Transport, heat and freshwater fluxes within a diagnostic numerical model (FRAM). *J. Phys. Oceanogr.*, **22**, 452–464.

Semtner, A. J., 1974: An oceanic general circulation model with bottom topography. UCLA Department of Meteorology, Tech. Rep. No. 9, 99 pp.

——, and R. M. Chervin, 1992: Ocean general circulation from a global eddy-resolving model. *J. Geophys. Res.*, **97**(C4), 5493–5550.

Stevens, D. P., and V. O. Ivchenko, 1993: The zonal momentum balance in a realistic eddy resolving general circulation model of the Southern Ocean. Unpublished manuscript.

Straub, D. N., 1992: On the transport and angular momentum balance of channel models of the Antarctic Circumpolar Current. *J. Phys. Oceanogr.*, **22**, 776–782.

Webb, D. J., 1993: A simple model of the effect of the Kerguelen Plateau on the strength of the Antarctic Circumpolar Current. *Geophys. Astrophys. Fluid Dyn.*, in press.